Clinical Hemorheology and Microcirculation 86 (2024) 263–273
DOI 10.3233/CH-249103
IOS Press

Novel high-resolution contrast agent ultrasound techniques HiFR CEUS and SR CEUS in combination with shear wave elastography, fat assessment and viscosity of liver parenchymal changes and tumors

Ernst Michael Jung[a], Ulrich Kaiser[b,*], Wolfgang Herr[b], Christian Stroszczynski[a] and Friedrich Jung[c]

[a]*Interdisciplinary Ultrasound Department, Institute of Diagnostic Radiology, University Hospital Regensburg, Regensburg, Germany*

[b]*Clinic and Polyclinic for Internal Medicine III, University Hospital Regensburg, Regensburg, Germany*

[c]*Molecular Cell Biology, Institute of Biotechnology, Brandenburg University of Technology, Senftenberg, Germany*

Abstract.

BACKGROUND: The continuous development of ultrasound techniques increasingly enables better description and visualization of unclear lesions. New ultrasound systems must be evaluated with regard to all these diagnostic possibilities.

METHODS: A multifrequency C1-7 convex probe (SC7-1M) with the new high-end system Resona A20 Series was used. Modern technologies, including HiFR CEUS, SR CEUS and multimodal tissue imaging with shear wave elastography (SWE), fat evaluation and viscosity measurements (M-Ref) were applied.

RESULTS: Of $n = 70$ (mean value 48,3 years $\pm$ 20,3 years, range 18–84 years) cases examined, a definitive diagnosis could be made in $n = 67$ cases, confirmed by reference imaging and/or follow-up. Of these, $n = 22$ cases were malignant changes (HCC (hepatocellular carcinoma) $n = 9$, CCC (cholangiocellular carcinoma) $n = 3$, metastases of colorectal carcinomas or recurrences of HCC $n = 10$). In all 12 cases of HCC or CCC, the elastography measurements using the shear wave technique (with values >2 m/s to 3.7 m/s) showed mean values of 2.3 ± 0.31 m/s and a degree of fibrosis of F2 to F4. In $n = 14$ cases, changes in the fat measurement (range 0.51 to 0.72 dB/cm/MHz, mean values 0.58 ± 0.12 dB/cm/MHz) in the sense of proportional fatty changes in the liver were detected. In the 4 cases of localized fat distribution disorders, the values were >0.7 dB/cm/MHz in the sense of significant fatty deposits in the remaining liver tissue. Relevant changes in the viscosity measurements with values >1.8 kPa were found in $n = 31$ cases, in $n = 5$ cases of cystic lesions with partially sclerosing cholangitis, in $n = 13$ cases of malignant lesions and in $n = 9$ cases post-interventionally, but also in $n = 4$ cases of benign foci with additional systemic inflammation.

CONCLUSIONS: The results are promising and show a new quality of ultrasound-based liver diagnostics. However, there is a need for further investigations with regard to the individual aspects, preferably on a multi-center basis.

Keywords: Multimodal liver tissue imaging (M-Ref), UMA, HiFR CEUS, SR CEUS, elastography, fat evaluation, viscosity

*Corresponding author: Kaiser Ulrich, Clinic and Polyclinic for Internal Medicine III, University Hospital Regensburg, Franz-Josef-Strauß Allee 11, 93053 Regensburg, Germany. E-mail: ulrich.kaiser@ukr.de.

ISSN 1386-0291/$35.00

1. Introduction

Modern ultrasound diagnostics includes a variety of imaging modalities that together provide comprehensive multimodal diagnostics [1, 2]. This includes high-resolution detailed analysis, comprehensive assessment of morphology, localization and characterization of lesions and dynamic macro- and microvascularization. Ultrasound examinations of the liver are among the most commonly performed: These includes a comprehensive detailed analysis of anatomy, morphology, vascularization, tissue compaction or steatosis, microcirculation and dynamic macro- and microcirculation [3–11]. In addition, contrast-enhanced computed tomography (CT), magnetic resonance imaging (MRI) and positron emission topography (PET) or PET CT must be performed for reliable diagnosis of benign and malignant lesions. In summary, this approach should make it possible to anticipate the morphology corresponding to a histopathological examination using multimodal ultrasound [12–16].

Multimodal ultrasound uses the latest matrix probes, mostly convex probes from 1 to 7 MHz, high-resolution B-mode techniques, color-coded duplex sonography CCDS, power mode (PD), elastography with strain and shear wave technology and contrast-enhanced ultrasound CEUS. In addition, new ultrasound techniques are now available to assess fat content by recording the attenuation and to estimate the viscosity with ultrasound are now also possible [1, 17, 18]. CEUS is being expanded to include high-resolution techniques such as HiFR CEUS or SR CEUS [2]. In addition, perfusion analysis using time-intensity curve TIC analysis and parametric false color are now available. All these imaging techniques provide measurements and require tabular documentation. Digital raw data or DICOM files with PACS connectivity allow comprehensive multimodal case analysis. The best possible treatment decision can then be made in interdisciplinary case conferences. This also includes the planning of surgery or interventions for malignant liver lesions. CEUS was optimized with M-Ref, which was separated into: RLBMap as quality indicator, STE as fibrosis, USAT as fat evaluation, STVi as viscosity.

Novel ultrasound systems need to be evaluated with regard for all these diagnostic capabilities. For this purpose, a novel high-end system A20 Mindray system was used with parallel imaging of elastography, fat assessment and viscosity and the high-resolution CEUS (HiFR) techniques SR CEUS and HiFR CEUS with parametric false-color analysis and, if possible, also TIC analysis [19–21].

Fig. 1. Inhomogeneous liver tissue with signs of cirrhosis in B-mode. Measurements with the multimodal imaging of the M-Ref show clearly increased fibrosis values with a mean of 2.7 m/s, a certain inflammatory reaction with viscosity values of 3.03 Pa·s on average and normal fat values of 0.4 dB/cm/MHz on average.

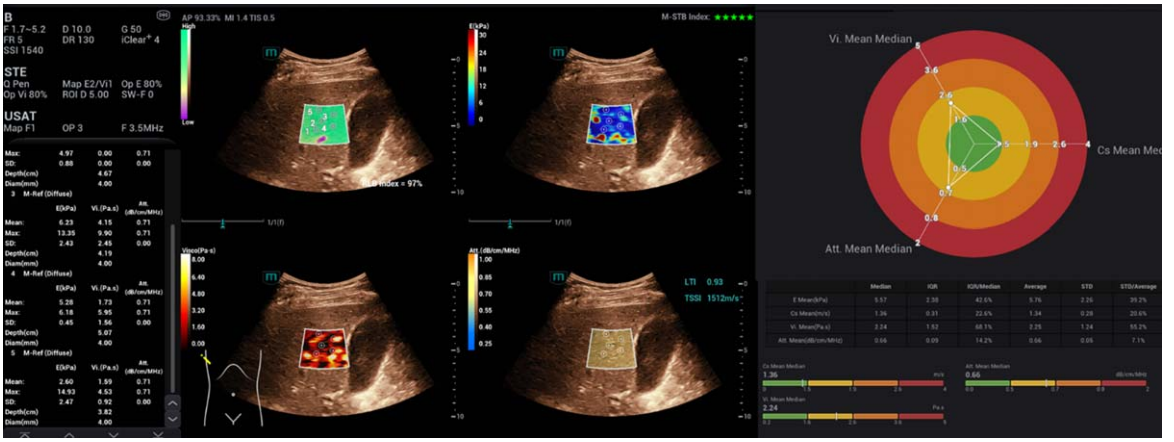

Fig. 2. Echogenic liver with smooth surface. Indication of steatosis in B-mode. Multimodal imaging with M-Ref with proportionally increased fat measurements with an average of 0.66 dB/cm/MHz. Normal measured values for the fibrosis measurements with an average of 1.36 m/s. Proportional increase in viscosity measurements with 2.24 Pa·s with known inflammatory reaction in the small pelvis.

The aim of the study was to investigate at the first time the extent to which these new multimodal capabilities of a new high-end ultrasound system allow a decisive diagnosis of morphological examinations, vascular and tumor changes in the liver in correlation with other cross-sectional imaging techniques or histology?

2. Material and methods

All examinations were performed by an experienced examiner (>3000 examinations/year, >20 years) using a high-end ultrasound machine (Mindray/Resona A20) with a convex probe from 1 to 7 MHz (SC7-1M). Requests for ultrasound examinations were made based on tumor board decisions. Written informed consent was available for CEUS examinations in all cases. The CEUS liver diagnostics comply with the EFSUM Guidelines as on-label use [3]. A positive ethics vote of the local ethics committee (as parts of the DEGUM IV study) is available [5].

Possible liver lesions were measured in B-mode and macrovascularization was documented with color-coded Doppler sonography (CCDS) and artifact-optimized imaging in high-resolution (HR) mode and with the option of glazing with micro flow methods, additionally adapted to low flow. The documentation was carried out using short cine loops and single frames. All new flow options were available under the function UMA. A wheel spoke pattern was considered typical for focal nodular hyperplasia (FNH) [22].

The evaluation of the liver parenchyma with regard to echogenicity was performed in comparison to the healthiest possible kidney parenchyma and was measurable in this respect under the function hepatorenal index (HRI+) as an index with ideal values up to 1. With color-coded elastography, the shear wave velocity was to be measured in the area of circular, individually adjustable regions of interest (ROI) in kPa or m/s. In this case, values <1.4 m/s were target values for healthy parenchyma.

In addition, a focused measurement was performed at a depth of 2 to 4 cm from the capsule using the STQ technique. At least 10 measurements were acquired, if possible outside vessels, not at bile ducts and in respiratory arrest. For this purpose, a quality indicator of maximum 5 green stars was available for orientation. Values of 1.4 m/s to 2.6 m/s were considered indicative of increasing fibrosis from F1 to F4. Higher values were considered to be evidence of cirrhosis.

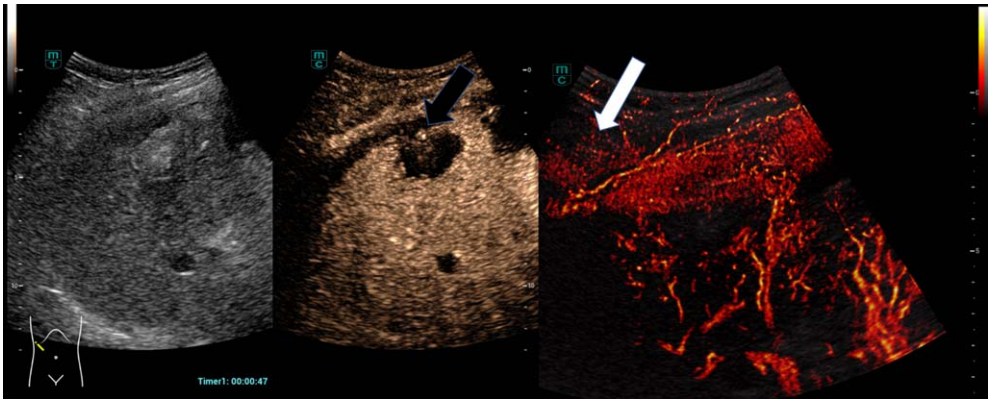

Fig. 3. Postoperative control after liver tumor resection with bolus administration of 2 ml SonoVue® i.v. with perihepatic fluid with low contrast agent transfer in superresolution CEUS (SR CEUS, right, white arrow). Avascular defect subcapsular in HiFR CEUS mode (black arrow, left). Noticeably increased capillary hypercirculation at the capsule. SR CEUS shows irregular vessels in cirrhosis.

With 2 additional tools, the degree of possible steatosis could be measured with documentation of possible artifact overlay and assessment in Liver texture index (LTI) mode for additional possible inflammatory changes. All liver parenchyma measurements were performed at a depth of 1 to a maximum of 5 cm, if possible, without recording vascular structures while avoiding motion and respiratory artifacts. Overall, a summary evaluation was possible under the USAT function (USAT, LTI, HRI+).

For the fat measurements, up to 10 individual measurements were targeted. Ideal values were measurements up to 0.5 dB/cm/MHz. Values >0.8 dB/cm/MHz were indicated of measured values of a clear steatosis.

Contrast enhanced ultrasonography (CEUS) was used to clarify non-cyst focal liver lesions. As a bolus of 1 to 2.4 ml i.v. of sulphur-hexafluoride microbubbles (SonoVue®, Bracco, Italy) with bolus administration of 10 ml NaCL was injected via cubital vein, the main lesion to be assessed was examined digitally as cine loops in DICOM format with respect to microvascularization [3]. Following a low mechanical index (MI) technique (MI < 0.15), low MI penetration depth was frequency adapted via general (GEN), resolution (RES) or penetration (PEN) function. Perfusion evaluation with false color and time intensity curve (TIC) analysis was then performed from the up to 60 s capturing approach with onset of possible wash out in the early portal venous phase. Parametrically, 10 s from the arterial insufflation were coded in false colors. Red and orange imply strongly hyper-vascularized portions, yellow moderate perfusion, green and blue low. A regular pattern typically appears in benign lesions, such as nodular from the margin in hemangiomas, homogeneous in fat distribution disorders, radicular from the center in FNH, from margin to center in adenomas [3, 4, 8, 22].

The main criteria for characterization of malignant lesions were irregular arterial microvascularization in CEUS, almost chaotic pattern in HCC, and wash out increasing to late phase from 3 to 5 min [3–6, 16, 18, 23].

These wash-out kinetics were recorded with short cine loops of 10 s over the entire liver, every 60 s if possible.

Measurement parameters of the TIC analysis were time to peak (TTP), peak enhancement, mean transit time (mTT) and area under the curve (AUC). These can be stored in a protocol [19, 20, 24]. Benign changes typically demonstrate a rather continuous increase of the contrast enhancement of the lesion until it is aligned with the surrounding area. Malignant lesion exhibits micro shunts with irregular hypervascularization, rapid curve rises and then wash out with curve flattening. Post ablation

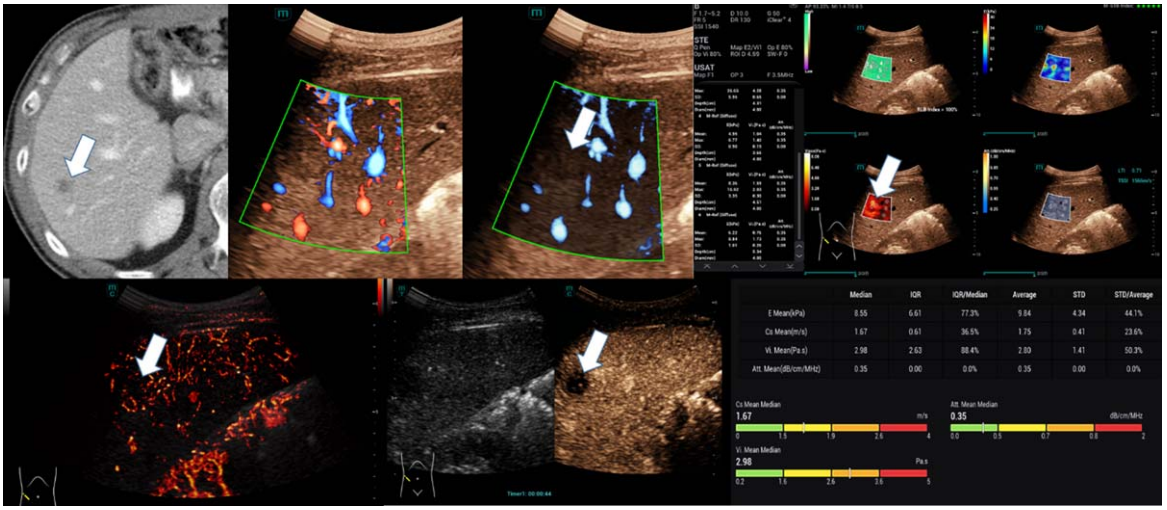

Fig. 4. Small lesion in the right lobe of the liver in the contrast-enhanced CT (white arrow), possibly cyst in AEG tumor. Regular vascular pattern in SR CEUS and wash out in HiFR CEUS as criteria of a malignant focus, a metastasis. Multimodal imaging with UMA and M-Ref, including detection of increased stiffness in shear wave elastography and increased viscosity of the malignant lesion. Examination with SC7-1U convex probe and 1.5 ml SonoVue® as bolus.

defects or scars after tumor resection should be avascular. Hooke's Law and Newtonian Fluid Laws formed the basis for the measurement of viscosity.

3. Results

Of the $n = 70$ cases examined (mean value 48,3 years, standard deviation 20,3 years, range 18 – 84 years), a definitive diagnosis could be made in 67/70 cases using multimodal imaging with the C1-7 convex probe with the new high-end system (Resona A20), confirmed by reference imaging and/or follow-up. Of these, $n = 22$ cases were malignant changes: $n = 9$ were HCC (hepatocellular carcinoma), $n = 3$ were CCC (cholangiocellular carcinoma) and $n = 10$ were metastases of colorectal carcinomas or recurrences of HCC.

Of the 29 cases of benign lesions, $n = 12$ were complicated, proportionally septated cystic lesions, $n = 8$ were typical or partially thrombosed haemangiomas, $n = 5$ were FNH (focal nodular hyperplasia) and $n = 4$ were low-echo fat distribution disorders near the gallbladder site with echo-rich steatosis.

In $n = 15$ cases, these were controls after various ablation treatments of malignant tumors (microwave ablation (MWA), electroporation (IRE) or electrochemotherapy (ECT)). In $n = 12$ cases, there was complete devascularization of the previously vascularized lesions. In $n = 3$ cases, the finding of irregular, partially irregular hypovascularized changes had to be reported with the need for a follow-up check in 3 months. This resulted in the finding of marginal recurrences up to a maximum of 10 mm or new small tumor foci in the marginal area in the CEUS and with the reference imaging. Only in the follow-up were these small tumor foci found to have a diagnostic wash out indicating malignancy. The ablations were performed on tumors >3.5 cm in diameter.

In $n = 4$ cases of Osler's disease, micro-shunts were detected particularly centrally and peripherally in segment VIII, $n = 2$ of which were already central. In these cases of vascular changes, also with high flow angiomas in $n = 2$ cases, the use of UMA proved to be helpful, whereby the angiomas could only be visualized in terms of localization and extent with CEUS and SR CEUS.

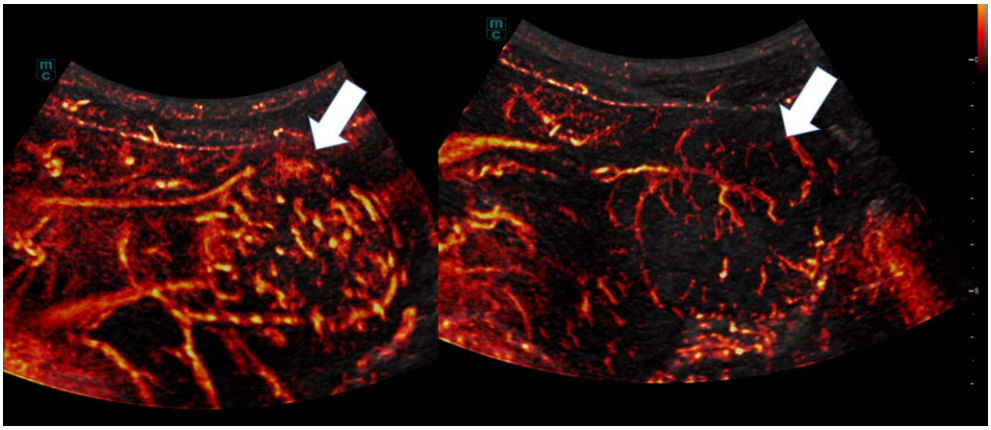

Fig. 5. Lesion of the left lobe of the liver in B-mode. Regular vascular pattern in SR CEUS as a criterion for a benign lesion. Wheel spoke pattern as a typical finding of focal nodular hyperplasia. Examination with SC 7-1U convex probe and 1.5 ml SonoVue® as a bolus.

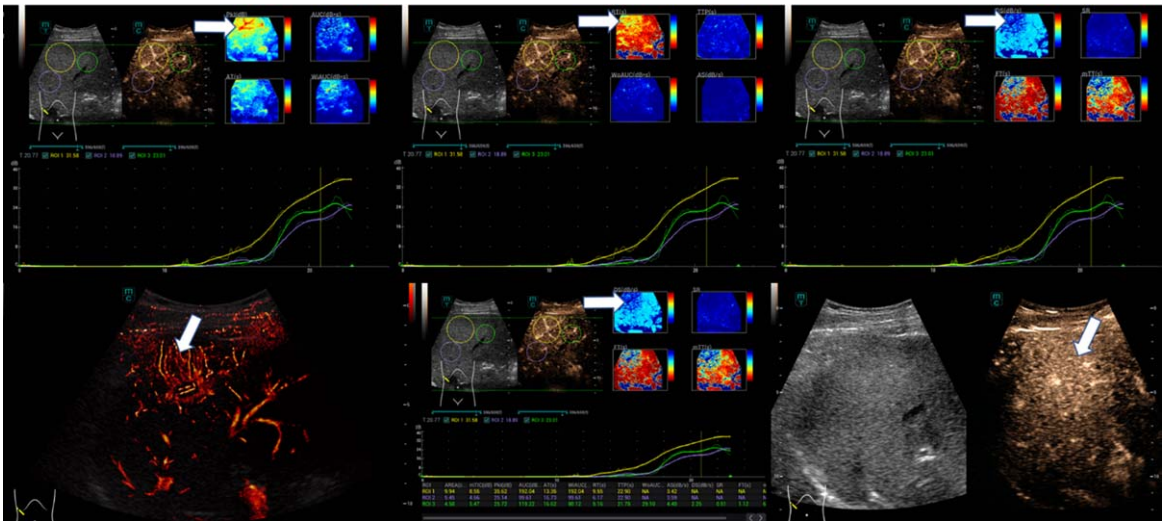

Fig. 6. Multimodal CEUS imaging to detect a liver lesion in segment VIII (white arrow). In HiFR CEUS almost equal contrast to the liver and in SR CEUS regular vascular pattern. Rapid enhancement in the time intensity curve (TIC) in the early arterial phase. Good delineation of the lesion in the color map, especially with the depiction of the PEAK, the mean transit time (mTT) and the rise time (RT). The lesion was not recognizable in the B-mode.

The importance of SR CEUS lay in the clear detection of regular arterial vascularization in benign lesions or vascular changes and irregular early microvascularization in malignant lesions. Typical for shunting was an early segmental arterial contrast and rapid transition into the portal venous and venous vascular system.

In hemangiomas and atypical hemangiomas, a nodular enhancement was found from the edge to the center. In FNH, an orderly, mostly spoke-like pattern from the center to the edge. Malignant hemangiomas and metastases showed irregular enhancement from the edge to the center. In HCC and CCC, chaotic central irregular vessels were found in some cases. Ablation defects and non-tumorous cysts should show as little enhancement as possible, or only slightly contrasted membranes <2 mm after IRE. In the case of inflammation, persistent septal and marginal contrast was typical. In all

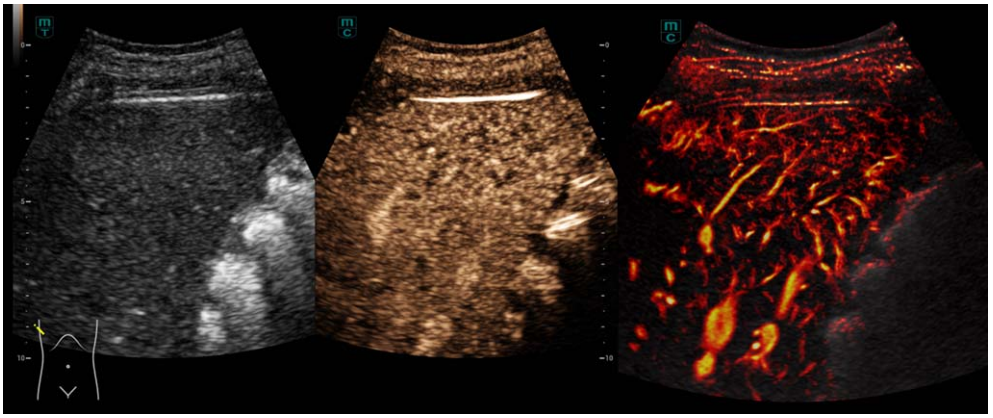

Fig. 7. After bolus administration of 1.5 ml SonoVue® i.v.: rapid and homogeneous contrast agent enhancement of the liver with regular vascular pattern in SR CEUS (right image) and low parenchymal inhomogeneity in HiFR CEUS (left image).

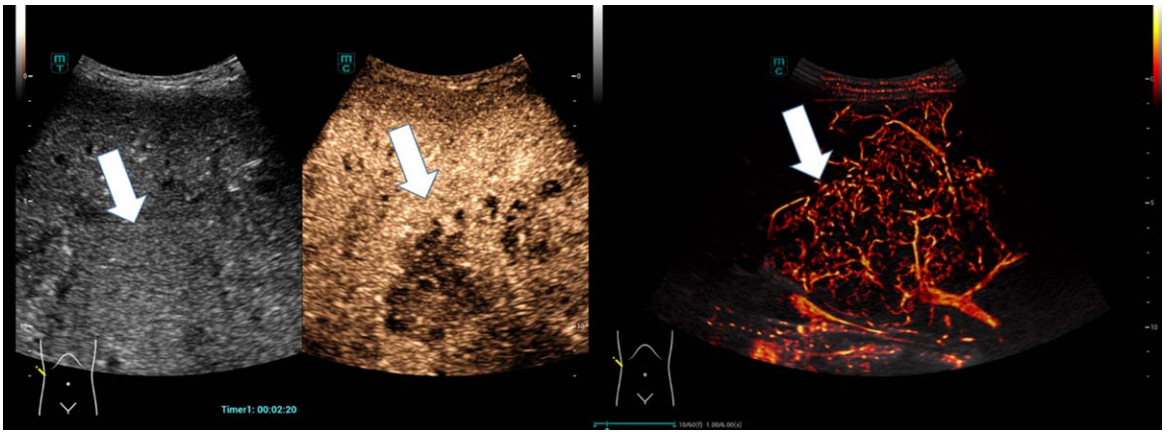

Fig. 8. Extensive echo-inhomogeneous mass of the right lobe of the liver in B-mode (white arrow). Irregular contrast in HiFR CEUS. Clear neovascularization in SR CEUS with irregular malignant tumor vessels. Findings of a highly proliferating hepatocellular carcinoma (HCC). Examination with SC 7-1U convex probe and 1.5 ml SonoVue® as a bolus.

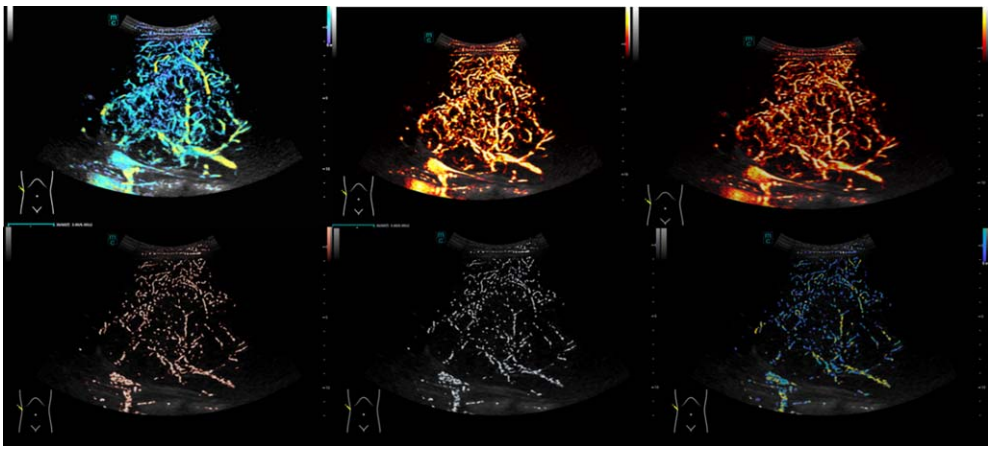

Fig. 9. Neovascularization in HCC: right liver lobe in SR CEUS with irregular malignant tumor vessels. Findings of a highly proliferating hepatocellular carcinoma (HCC). Examination with SC7-1U convex probe and 1.5 ml SonoVue® as a bolus. Post-processing with different color scaling.

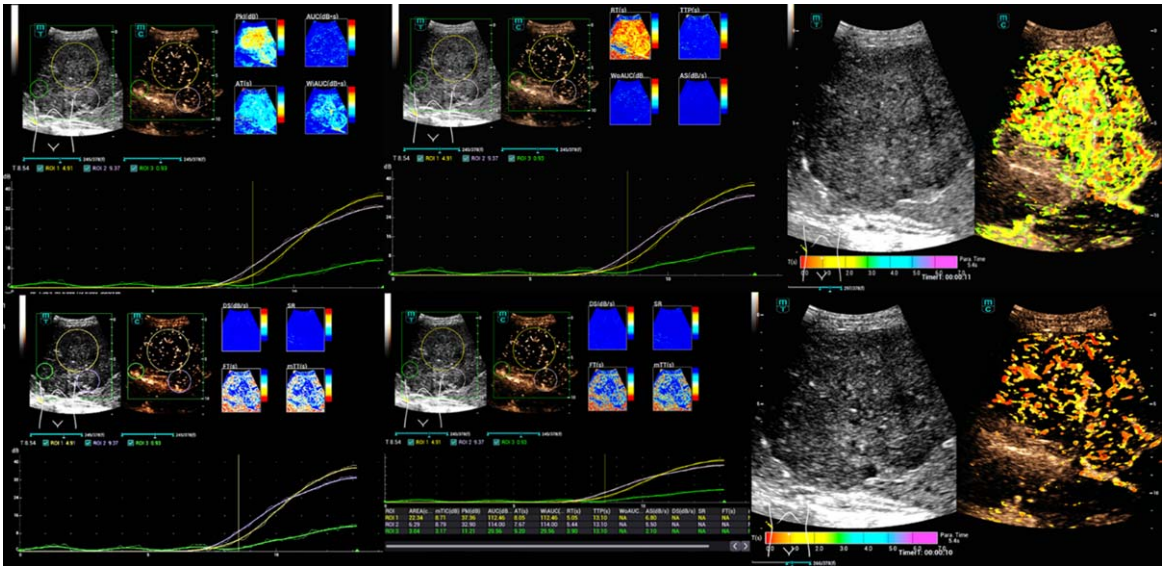

Fig. 10. Time intensity curve analysis (TIC, CEUS perfusion and parametric CEUS) for dynamic assessment of microvascularization and neovascularization in HCC right liver lobe in SR CEUS with irregular malignant tumor vessels. Findings of a highly proliferating hepatocellular carcinoma (HCC). Examination with SC7-1U convex probe and 1.5 ml SonoVue® as a bolus.

cases, however, only the wash-out dynamic with additional CEUS and, in the case of lesions <12 mm, especially HiFR CEUS in the late phase up to 6 minutes could be used to decide whether malignant or not on the basis of a possible wash-out.

In all $n = 12$ cases of HCC or CCC, the elastography measurements using the shear wave technique with values >2 m/s to 3.7 m/s showed mean values of 2.3 ± 0.31 m/s and a degree of fibrosis of F2 to F4. In $n = 7$ cases there were increases in viscosity and only in $n = 2$ cases there were proportional increases in fat values of up to 0.64 dB/cm/MHz.

Of the $n = 15$ cases of post-interventional controls, the degrees of fibrosis were in the range of F2 (from 1.59 to 2.3 m/s, mean value 1.88 ± 0.24 m/s). In $n = 9$ cases, there were increases in viscosity. In $n = 12$ cases there were changes in the fat measurement (0.51 to 0.78 dB/cm/MHz, mean values 0.68 ± 0.15 dB/cm/MHz) in the sense of massive fatty liver. In the $n = 29$ cases with benign lesions and complicated cystic lesions and the $n = 4$ vascular changes in M. Osler, the measurements of the degree of fibrosis ranged from normal values <1.4 m/s to a degree of fibrosis of F1 with values of 1.93 m/s, mean value 1.51 ± 0.27 m/s. In $n = 5$ cases there may be increases in viscosity. In $n = 14$ cases, changes in the fat measurement (0.51 to 0.72 dB/cm/MHz, mean values 0.58 ± 0.12 dB/cm/MHz) in the sense of proportional fatty changes in the liver. In the $n = 4$ cases of localized fat distribution disorders, the values were >0.7 dB/cm/MHz in the sense of significant fatty deposits in the remaining liver tissue.

Relevant changes in the viscosity measurements with values >1.8 Pa·s were found in $n = 31$ cases: in $n = 5$ cases of cystic lesions with partially sclerosing cholangitis, in $n = 13$ cases of malignant lesions, in $n = 9$ cases post-interventionally, but also in $n = 4$ cases of benign foci with additional systemic inflammation.

4. Discussion

The establishment of a new ultrasound system involves the application of new diagnostic tools to common clinical problems. Most commonly, multimodal ultrasound is used for comprehensive

ultrasound parenchymal analysis of the liver, assessment of vascular changes in the liver, and detection and characterization of tumor changes in the liver. In all cases studied, multimodal imaging with high-resolution B-mode, vascular analysis with CCDS, Power Doppler and UMA, parallel with shear wave elastography, fat assessment and viscosity and dynamic analysis of the microcirculation with HiFR CEUS and SR CEUS enabled a comprehensive diagnosis [2, 18, 24].

The classification into different degrees of liver fibrosis up to cirrhosis correlated in all cases with baseline measurements and characterization from CT and MRI. In biopsies, F4 fibrosis was usually classified as cirrhosis (degree of fatty degeneration >0.7 dB/cm/MHz). Increased viscosity values greater than 2 Pa·s were found in active inflammation, active hepatitis or pronounced tumors [25, 26]. Multimodal ultrasound parenchymal diagnostics proved to be particularly useful in the follow-up of hepatitis B under maintenance therapy and NSH. Fat distribution abnormalities can be quickly analyzed as benign. If pulsations through the heart or vessels are avoided, the measurements can be carried out quickly and with high image quality in all cases up to 20 individual values, characterization with homogeneous windows and 5 stars in the integrated quality control.

Initial preliminary studies on HiFR CEUS are confirmed by the current results [2, 18, 24]. Focal parenchymal changes can be clearly differentiated from benign solid and malignant tumors. On the other hand, the differentiation of an adenoma from an HCC can be difficult with partial wash-out centrally, but this is also true with liver-specific MRI [5, 6, 16, 18, 23]. Follow-up without any change in findings was helpful if no biopsy was performed. The detection of small HCC foci, or in general, tumor foci with irregular hypervascularization without wash-out can also be difficult, especially in the case of subdiaphragmatic localization of segment VIII, IVa, marked steatosis and meteorism with colonic interposition. SR CEUS can be used to visualize the irregular vascular architecture of malignant tumors, similar to a super-selective angiography in DSA. These changes have been shown to be particularly impressive in intrahepatic micro- and macro-shunts, Osler's disease and devascularization following intervention or surgery [21, 27]. At present, SR CEUS is best suited for a penetration depth of up to 10 cm. HiFR CEUS can reach further and deeper regions in false color reconstruction. TIC perfusion is useful to assess the success of therapy. With complete ablation, defects should be avascular, with a near-zero line and no color coding on the color maps [19, 20, 28]. Time to peak (TTP), peak enhancement (PI), mean transit time (mTT) and rise time (RT) are particularly useful, as shown in preliminary studies [19–21, 24, 27, 29].

Limitations are that CEUS perfusion can't be performed simultaneously with SR CEUS and the parameters require optimal measurements without large movement artifacts with experienced examiners [30].

For malignant lesions, wash-out in the late phase is crucial and can be easily detected with HiFR CEUS up to 6 minutes after injection. Often only 1 to 1.5 ml of ultrasound contrast agent is required as a bolus, without risk to the kidneys, as shown in previous studies [3, 5, 8, 15].

Preliminary studies have already shown that HR-Flow and Glazing-Flow can optimize CCDS and Power Doppler by reducing artefacts and improving dynamic flow detection without relevant angular artefacts for microvascularization of the liver, the portal vein intrahepatic and extrahepatic portal vein, hepatic veins and the hepatic artery [31]. With the new p-UMA and s-UMA modalities, it is now even possible to detect capsule vessels without contrast medium.

5. Conclusion

This study is the first experience of comprehensive multimodal ultrasound diagnostics using a novel high-performance ultrasound system. The results are extremely promising and show a new quality of ultrasound-based liver diagnostics. However, the results presented here need to be further evaluated with regard to the individual aspects, preferably on a multi-center basis.

References

[1] Jung EM, Dong Y, Jung F. Current aspects of multimodal ultrasound liver diagnostics using contrast-enhanced ultrasonography (CEUS), fat evaluation, fibrosis assessment, and perfusion analysis – An update. Clin Hemorheol Microcirc. 2023;83(2):181-93.

[2] Jung EM, Moran VO, Engel M, Krüger-Genge A, Stroszczynski C, Jung F. Modified contrast-enhanced ultrasonography with the new high-resolution examination technique of high frame rate contrast-enhanced ultrasound (HiFR-CEUS) for characterization of liver lesions: First results. Clin Hemorheol Microcirc. 2023;83(1):31-46.

[3] Dietrich CF, Nolsøe CP, Barr RG, Berzigotti A, Burns PN, Cantisani V, et al. Guidelines and Good Clinical Practice Recommendations for Contrast-Enhanced Ultrasound (CEUS) in the Liver-Update 2020 WFUMB in Cooperation with EFSUMB, AFSUMB, AIUM, and FLAUS. Ultrasound Med Biol. 2020;46(10):2579-604.

[4] Huang JY, Li JW, Lu Q, Luo Y, Lin L, Shi YJ, et al. Diagnostic accuracy of CEUS LI-RADS for the characterization of liver nodules 20mm or smaller in patients at risk for hepatocellular carcinoma. Radiology. 2020;294(2):329-39.

[5] Schellhaas B, Bernatik T, Bohle W, Borowitzka F, Chang J, Dietrich CF, et al. Contrast-enhanced ultrasound algorithms (CEUS-LIRADS/ESCULAP) for the noninvasive diagnosis of hepatocellular carcinoma – A prospective multicenter DEGUM study. Ultraschall Med. 2021;42(2):178-86.

[6] Strobel D, Jung EM, Ziesch M, Praktiknjo M, Link A, Dietrich CF, et al. Real-life assessment of standardized contrast-enhanced ultrasound (CEUS) and CEUS algorithms (CEUS LI-RADS®/ESCULAP) in hepatic nodules in cirrhotic patients-a prospective multicenter study. Eur Radiol. 2021;31(10):7614-25.

[7] Sporea I, Badea R, Popescu A, Spârchez Z, Sirli RL, Dănilă M, et al. Contrast-enhanced ultrasound (CEUS) for the evaluation of focal liver lesions – a prospective multicenter study of its usefulness in clinical practice. Ultraschall Med. 2014;35(3):259-66.

[8] Seitz K, Strobel D, Bernatik T, Blank W, Friedrich-Rust M, Herbay A, et al. Contrast-Enhanced Ultrasound (CEUS) for the characterization of focal liver lesions – prospective comparison in clinical practice: CEUS vs. CT (DEGUM multicenter trial). Parts of this manuscript were presented at the Ultrasound Dreiländertreffen 2008, Davos. Ultraschall Med. 2009;30(4):383-9.

[9] Zhao Q, Ji Z, Chen Y, Wang K, Qiu Y, Tian X, et al. Contrast-enhanced ultrasound features of hepatic sarcomatoid carcinoma different from hepatocellular carcinoma. Clin Hemorheol Microcirc. 2023.

[10] Zhang W, Liu Y, Wu Q, Wei X, Liu B, Jiao Q, et al. Pitfalls and strategies of Sonazoid enhanced ultrasonography in differentiating metastatic and benign hepatic lesions. Clin Hemorheol Microcirc. 2023.

[11] Meitner-Schellhaas B, Jesper D, Goertz RS, Zundler S, Strobel D. Washout appearance of hepatocellular carcinomas using standardized contrast-enhanced ultrasound (CEUS) including an extended late phase observation – Real-world data from the prospective multicentre DEGUM study. Clin Hemorheol Microcirc. 2023;84(4):413-24.

[12] Rennert J, Grosse J, Einspieler I, Bäumler W, Stroszczynski C, Jung EM. Complementary imaging of ultrasound and PET/CT: A new opportunity? Clin Hemorheol Microcirc. 2021;79(1):39-54.

[13] Müller-Peltzer K, Rübenthaler J, Negrao de Figueiredo G, Clevert DA. CEUS-diagnosis of benign liver lesions. Radiologe. 2018;58(6):521-7.

[14] Strobel D, Bernatik T, Blank W, Schuler A, Greis C, Dietrich CF, et al. Diagnostic accuracy of CEUS in the differential diagnosis of small ($\leq$20 mm) and subcentimetric ($\leq$10 mm) focal liver lesions in comparison with histology. Results of the DEGUM multicenter trial. Ultraschall Med. 2011;32(6):593-7.

[15] Seitz K, Bernatik T, Strobel D, Blank W, Friedrich-Rust M, Strunk H, et al. Contrast-enhanced ultrasound (CEUS) for the characterization of focal liver lesions in clinical practice (DEGUM Multicenter Trial): CEUS vs. MRI–a prospective comparison in 269 patients. Ultraschall Med. 2010;31(5):492-9.

[16] Marschner CA, Zhang L, Schwarze V, Völckers W, Froelich MF, von Münchhausen N, et al. The diagnostic value of contrast-enhanced ultrasound (CEUS) for assessing hepatocellular carcinoma compared to histopathology; a retrospective single-center analysis of 119 patients 1. Clin Hemorheol Microcirc. 2020;76(4):453-8.

[17] Jung EM, Stroszczynski C, Jung F. Advanced multimodal imaging of solid thyroid lesions with artificial intelligence-optimized B-mode, elastography, and contrast-enhanced ultrasonography parametric and with perfusion imaging: Initial results. Clin Hemorheol Microcirc. 2023;84(2):227-36.

[18] Dong Y, Wang WP, Mao F, Zhang Q, Yang D, Tannapfel A, et al. Imaging features of fibrolamellar hepatocellular carcinoma with contrast-enhanced ultrasound. Ultraschall Med. 2021;42(3):306-13.

[19] Wiesinger I, Jung F, Jung EM. Contrast-enhanced ultrasound (CEUS) and perfusion imaging using VueBox®. Clin Hemorheol Microcirc. 2021;78(1):29-40.

[20] Jung EM, Weber MA, Wiesinger I. Contrast-enhanced ultrasound perfusion imaging of organs. Radiologe. 2021;61(Suppl 1):19-28.

[21] Schelker RC, Andorfer K, Putz F, Herr W, Jung EM. Identification of two distinct hereditary hemorrhagic telangiectasia patient subsets with different hepatic perfusion properties by combination of contrast-enhanced ultrasound (CEUS) with perfusion imaging quantification. PLoS One. 2019;14(4):e0215178.
[22] Şirli R, Sporea I, Popescu A, Dănilă M, Săndulescu DL, Săftoiu A, et al. Contrast-enhanced ultrasound for the assessment of focal nodular hyperplasia – results of a multicentre study. Med Ultrason. 2021;23(2):140-6.
[23] Wildner D, Bernatik T, Greis C, Seitz K, Neurath MF, Strobel D. CEUS in hepatocellular carcinoma and intrahepatic cholangiocellular carcinoma in 320 patients – early or late washout matters: a subanalysis of the DEGUM multicenter trial. Ultraschall Med. 2015;36(2):132-9.
[24] Dong Y, Qiu Y, Yang D, Yu L, Zuo D, Zhang Q, et al. Potential application of dynamic contrast enhanced ultrasound in predicting microvascular invasion of hepatocellular carcinoma. Clin Hemorheol Microcirc. 2021;77(4):461-9.
[25] Săftoiu A, Gilja OH, Sidhu PS, Dietrich CF, Cantisani V, Amy D, et al. The EFSUMB Guidelines and Recommendations for the Clinical Practice of Elastography in Non-Hepatic Applications: Update 2018. Ultraschall Med. 2019;40(4):425-53.
[26] Popa A, Bende F, Şirli R, Popescu A, Bâldea V, Lupuşoru R, et al. Quantification of liver fibrosis, steatosis, and viscosity using multiparametric ultrasound in patients with non-alcoholic liver disease: A "Real-Life" cohort study. Diagnostics (Basel). 2021;11(5).
[27] Schelker RC, Barreiros AP, Hart C, Herr W, Jung EM. Macro- and microcirculation patterns of intrahepatic blood flow changes in patients with hereditary hemorrhagic telangiectasia. World J Gastroenterol. 2017;23(3):486-95.
[28] Liu F, Liu D, Wang K, Xie X, Su L, Kuang M, et al. Deep learning radiomics based on contrast-enhanced ultrasound might optimize curative treatments for very-early or early-stage hepatocellular carcinoma patients. Liver Cancer. 2020;9(4):397-413.
[29] Bernatik T, Schuler A, Kunze G, Mauch M, Dietrich CF, Dirks K, et al. Benefit of contrast-enhanced ultrasound (CEUS) in the follow-up care of patients with colon cancer: A prospective multicenter study. Ultraschall Med. 2015;36(6):590-3.
[30] Putz FJ, Verloh N, Erlmeier A, Schelker RC, Schreyer AG, Hautmann MG, et al. Influence of limited examination conditions on contrast-enhanced sonography for characterising liver lesions. Clin Hemorheol Microcirc. 2019;71(2):267-76.
[31] Jung EM, Kammerer S, Brandenstein M, Putz FJ, Stroszczynski C, Jung F. High resolution flow (HR Flow) and Glazing Flow in cases of hepatic flow changes: Comparison to color-coded Doppler sonography (CCDS). Clin Hemorheol Microcirc. 2021;79(1):3-17.